arXiv:1603.01460v1 [cond-mat.stat-mech] 4 Mar 2016

Imaginary noise and parity conservation in the reaction $A + A \rightleftharpoons 0$

O. Deloubrière[1], L. Frachebourg[2], H.J. Hilhorst[1], and K. Kitahara[3]

[1]Laboratoire de Physique Théorique, Bâtiment 210
Université de Paris-Sud, 91405 Orsay cedex, France
[2] 11 rue Fendt, 1201 Genève, Switzerland
[3]Division of Natural Sciences, International Christian University
10-2 Osawa 3-chome, Mitaka-shi, Tokyo 181-8585, Japan

March 7, 2016

Abstract

The master equation for the reversible reaction $A + A \rightleftharpoons 0$ is considered in Poisson representation, where it is equivalent to a Langevin equation with imaginary noise for a complex stochastic variable ϕ. Such Langevin equations appear quite generally in field-theoretic treatments of reaction–diffusion problems. For this example we study the probability flow in the complex ϕ plane both analytically and by simulation. We show that this flow has various curious features that must be expected to occur similarly in other Langevin equations associated with reaction–diffusion problems.
PACS 05.40+j

LPT ORSAY 01/74
Laboratoire associé au Centre National de la Recherche Scientifique - UMR 8627

1 Introduction

Let there be a reacting chemical system with diffusing species $A, B, \ldots$ By a "chemical" master equation is meant one which governs the time evolution of the probability distribution of the particle numbers of these species. Under certain conditions such an equation is equivalent, via a "Poisson representation," to a Langevin equation with imaginary noise for space and time dependent fields $\phi_A(x,t)$, $\phi_B(x,t), \ldots$ This equivalence was first shown by Gardiner and coworkers (see [1]) and has reappeared [2] in field-theoretic treatments of reaction–diffusion problems as an outcome of the second-quantized formalism. Imaginary noise is typically (although not only) due to reaction processes whose reactants include two or more particles of the same species; it is a mathematical tool that helps in an elegant way to keep track of evolving probability distributions.

It is of interest to investigate such imaginary noise Langevin equations more closely. The motivation comes, for one part, from the intrinsic interest of a relatively unexplored type of equation, and for another part, from the hope that perhaps Monte Carlo simulation of a reaction–diffusion system in this new representation could turn out to be efficient. This latter idea is reinforced by the fact that the stochastic diffusive motion of the reacting particles becomes *deterministic* in the Poisson representation: The Langevin noise is exclusively due to the reaction processes.

One may therefore learn about imaginary noise even in the absence of diffusion. In this note we present a case study in which, for simplicity and in order to fully control all aspects of the problem, we will disregard diffusion except for a brief mention at the end. We will examine the single-species reversible reaction process

$$A + A \rightleftharpoons 0 \tag{1}$$

where the symbol "0" may represent an inert species. Its only parameter is the ratio λ of the forward $(0 \to 2A)$ to backward $(2A \to 0)$ reaction rates.

Several questions of interest may be investigated on this example. In general, reactions may or may not conserve the *parity* of the total particle number, with ensuing consequences for the critical behavior of a system (for an enlightening recent discussion see [3]). Hence one natural and nontrivial question here is how the parity conservaton of reaction (1) is reflected in the properties of the imaginary noise Langevin equation.

In its usual particle number representation the reaction (1) is of course fully understood and trivial. However, the corresponding Langevin equation, which is a stochastic ODE for a single function ("field") $\phi(t)$, has many curious features. These will be the focus of our interest here. We will see that not all of these features necessarily have their counterparts in physical properties, and will try to identify the role of each.

We mention some related work. The usual interest in the literature has been in the case $\lambda = 0$ (only particle annihilation) in the presence of diffusion (see *e.g.* Lee [4] and references therein); the main object of study then is the exponent of the power law decay to the zero density state. The two coupled Langevin equations for the reaction $A + A \rightleftharpoons C$ and $A + B \rightleftharpoons C$ with diffusion were studied in detail by Rey and Cardy [5]. They are interested in how the C particle densities approaches its equilibrium values for large times. Howard and Täuber [6] study various reaction–diffusion systems involving the process $A + A \to 0$ and subject to both imaginary and real noise, the latter being due to coupling to one or more other reaction processes. They are led to conclude that even in the presence of additional real noise the imaginary noise cannot be neglected.

In Sec. 2 we present the master equation and equivalent Langevin equation for the process (1). In Secs. 3-6 we address successively various aspects of the motion in the complex plane. In Secs. 7 and 8 we consider the limiting cases $\lambda \to \infty$ and $\lambda \to 0$, respectively. In Sec. 9 we investigate the possibility of alternative ways of simulating reaction–diffusion problems. We point out several difficulties and questions associated with simulating the time evolution of the Poisson variable ϕ. Some of the effects of an additional diffusion term are also briefly discussed.

2 Langevin equation with imaginary noise

For the process (1) the probability $P(n,t)$ of having n particles A at time t obeys the master equation

$$\begin{aligned}\frac{\mathrm{d}P(n,t)}{\mathrm{d}t} &= \tfrac{1}{2}(n+1)(n+2)P(n+2,t) - \tfrac{1}{2}n(n-1)P(n,t) \\ &\quad + \lambda\Big[P(n-2,t) - P(n,t)\Big] \qquad (n=0,1,2,\ldots)\end{aligned} \tag{2}$$

with the convention $P(-2,t) = P(-1,t) = 0$. Following Gardiner [1] one writes for $P(n,t)$ the Poisson representation

$$P(n,t) = \int\!\mathrm{d}x\int\!\mathrm{d}y\, F(x,y,t)\, p_{x+\mathrm{i}y}(n) \tag{3}$$

in which $p_\phi(n) = \phi^n \mathrm{e}^{-\phi}/n!$ is the Poisson distribution of parameter ϕ. It is a true probability only for real positive ϕ and a "quasi-probability" for arbitrary complex $\phi = x + \mathrm{i}y$. For any $P(n,t)$ there exists a nonunique $F(x,y,t)$ such that (3) holds; one may impose the additional requirement that F be real and nonnegative, but even so it is nonunique. In any case it is normalized such that $\int\!\mathrm{d}x\int\!\mathrm{d}y\, F(x,y,t) = 1$.

The equivalence between the Poisson representation method [1] and the second quantized formalism [7, 8, 9] was first pointed out by Droz and McKane [10], who however avoid discussing Langevin equations. By either approach one shows that $P(n,t)$ defined by (3) satisfies the master equation (2) if $F(x,y,t)$ is the probablity density of a variable $\phi = x + \mathrm{i}y$ obeying the Langevin equation

$$\frac{\mathrm{d}\phi}{\mathrm{d}t} = 2\lambda - \phi^2 + \sqrt{2\lambda - \phi^2}\;\zeta(t) \qquad [\,\mathrm{I}\,] \tag{4}$$

Here $\zeta(t)$ is Gaussian white noise of autocorrelation $\langle\zeta(t)\zeta(t')\rangle = \delta(t-t')$ and $[\,\mathrm{I}\,]$ indicates the Itô interpretation [1, 11, 13]. Equation (4) is the subject of the present study. It derives it interest from the fact that the noise term is complex whenever ϕ is outside the real interval $[-\sqrt{2\lambda}, \sqrt{2\lambda}]$.

The field-theoretical approach of Ref. [2] deals with the case $\lambda = 0$ and the noise term in the Langevin equation there appears as $\xi(t) = \mathrm{i}\phi(t)\zeta(t)$. Hence $\xi(t)$ is Gaussian white noise with

$$\langle\xi(t)\xi(t')\rangle = -\phi^2\delta(t-t') \tag{5}$$

Because of the minus sign on the RHS of (5) and perhaps because of the suggestive factor $-\phi^2$, the noise is usually referred to as "imaginary." Of course the noise term as well as the other terms in the Langevin equation (4) are generically complex.

The time dependent averages calculated from the master equation (2) are related to those found from the Langevin equation (4) by [1]

$$\langle\phi^k\rangle = \langle n(n-1)\ldots(n-k+1)\rangle \qquad (k=0,1,2,\ldots) \tag{6}$$

where the average on the LHS is with respect to F and that on the RHS with respect to P. Although the average of primary interest, $\langle n\rangle$, is equal to $\langle\phi\rangle$, it needs to be stressed [2, 6] that ϕ is not itself a physical variable.

Fokker-Planck equation. The Langevin equation (4), separated into its real and imaginary parts, is equivalent [1, 11] to a Fokker-Planck (FP) equation for the probability density $F(x,y,t)$. We will occasionally refer to this FP equation, but do not need its explicit general form. Let us consider, however, the special case of an initial value $\phi(0)$ in the interval $[-\sqrt{2\lambda}, \sqrt{2\lambda}]$. Equation (4) shows that then $\phi(t)$ remains confined to this section of the real axis at all $t > 0$. Upon denoting the time dependent probability density of $\phi = x + \mathrm{i}y$ on this interval by $F_1(x,t)$ we get from (4) the equivalent FP equation

$$\frac{\partial F_1(x,t)}{\partial t} = \Big[\frac{\partial}{\partial x} - \tfrac{1}{2}\frac{\partial^2}{\partial x^2}\Big]\,(2\lambda - x^2)\,F_1(x,t) \tag{7}$$

which will be referred to in Secs. 6 and 7.

3 Parity conservation

The master equation (2) leaves the subspaces of even and odd n invariant, so that $\mathcal{P} \equiv \langle (-1)^n \rangle$ is a constant of the motion. Upon evaluating this average by inserting for P its Poisson representation (3) one finds that

$$\langle (-1)^n \rangle = \langle \mathrm{e}^{-2\phi} \rangle \tag{8}$$

which shows that $\langle \mathrm{e}^{-2\phi} \rangle$ is the corresponding constant of the motion in ϕ language. Within the second quantized formalism one may arrive at the same relation (8) at the cost of a somewhat greater algebraic effort [12].

It is of interest to show explicitly, starting from the Langevin equation (4), that $\langle \mathrm{e}^{-2\phi} \rangle$ is conserved. One may do so by transforming this equation to the new variable $\alpha = \mathrm{e}^{-2\phi}$. We recall that the Langevin-Itô equation $\mathrm{d}\phi/\mathrm{d}t = G(\phi) + H(\phi)\zeta(t)$ is equivalent to the Langevin-Stratonovich equation $\mathrm{d}\phi/\mathrm{d}t = G(\phi) - \frac{1}{2}H(\phi)\mathrm{d}H/\mathrm{d}\phi + H(\phi)\zeta(t)$, and that in the latter the unknown may be nonlinearly transformed according to the usual rules of algebra [1, 11]. Hence the Stratonovich ([S]) version of (4) is

$$\frac{\mathrm{d}\phi}{\mathrm{d}t} = 2\lambda - \phi(\phi - \tfrac{1}{2}) + \sqrt{2\lambda - \phi^2}\,\zeta(t) \qquad [\ \mathrm{S}\ ] \tag{9}$$

which, transformed to an equation for α and reconverted to Itô interpretation, yields

$$\frac{\mathrm{d}}{\mathrm{d}t}\mathrm{e}^{-2\phi} = 2\mathrm{e}^{-2\phi}\sqrt{2\lambda - \phi^2}\,\zeta(t) \qquad [\ \mathrm{I}\ ] \tag{10}$$

In the Itô interpretation the noise $\zeta(t)$ is independent of $\phi(t)$ and so upon averaging (10) over $\zeta(t)$ the RHS vanishes, after which an average with respect to $F(x, y, t)$ yields the parity conservation law.

4 Time evolution: General properties

We first comment on some general properties of the Langevin equation (4). These may be analyzed in terms of two sets of curves in the complex plane, exhibited in Fig. 1 for the particular parameter value $\lambda = 3$.

Diffusion curves. In any point of the complex plane the diffusive displacement (*i.e.* the displacement due to the noise term in (4)) is along a single direction. This means that the diffusion tensor in the equivalent FP equation for $F(x, y, t)$ has one zero eigenvalue, and therefore this FP equation is not generic. The zero eigenvalue becomes explicit in an appropriate set of coordinates, as we will show now.

Upon dividing (9) by $\sqrt{2\lambda - \phi^2}$ one finds

$$\frac{\mathrm{d}}{\mathrm{d}t}\,\arcsin\frac{\phi}{\sqrt{2\lambda}} = \frac{2\lambda - \phi(\phi - \frac{1}{2})}{\sqrt{2\lambda - \phi^2}} + \zeta(t) \tag{11}$$

Then setting $\arcsin(\phi/\sqrt{2\lambda}) \equiv \mathcal{Q}(x, y) - \mathrm{i}\mathcal{R}(x, y)$ and taking real and imaginary parts of (11) one gets an expression for $\mathrm{d}\mathcal{Q}/\mathrm{d}t$ which contains the noise $\zeta(t)$ and one for $\mathrm{d}\mathcal{R}/\mathrm{d}t$ which shows that $\mathcal{R}$ is unaffected by the noise. The diffusion therefore operates only along curves $\mathcal{R}(x, y) = C$, where C is a constant. From the explicit expression of $\mathcal{R}(x, y)$ one finds that this collection of "diffusion curves" is given by

$$\Big|\frac{1 - \sqrt{1 - 2\lambda/\phi^2}}{1 + \sqrt{1 - 2\lambda/\phi^2}}\Big| = \mathrm{e}^{-2C} \qquad (C \geq 0) \tag{12}$$

The curves, shown in Fig. 1, are symmetric under reflection with respect to the x and y axis. They constitute a nested collection of closed contours that go around the real interval $[-\sqrt{2\lambda}, \sqrt{2\lambda}]$; there is one such contour through each point of the complex plane. The degenerate contour $C = 0$ coincides with $[-\sqrt{2\lambda}, \sqrt{2\lambda}]$.

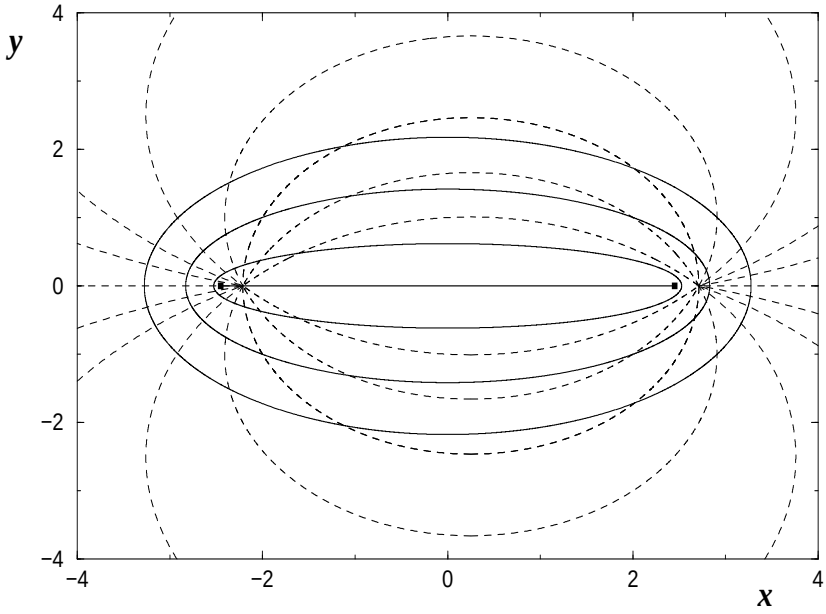

Figure 1: Diffusion curves (solid lines, symmetric about $x = 0$) and drift trajectories (dashed lines, symmetric about $x = \frac{1}{4}$) in the complex $\phi = x + \mathrm{i}y$ plane for various values of C and D in Eqs. (12) and (13), respectively, and for $\lambda = 3$. The interval $[-\sqrt{2\lambda}, \sqrt{2\lambda}]$ is bounded by the two filled squares. The drift trajectories all originate in a single point ϕ_- and terminate in a single point ϕ_+, both on the x axis (see text).

Drift trajectories. A second collection of curves is determined by the solutions of the drift equations, *i.e.* of (11) [or equivalently (9)] with ζ set equal to zero. We will refer to these curves as the "drift trajectories." They may be parametrized by an integration constant D and the sign of y, and are explicitly given by

$$(x - \tfrac{1}{4})^2 + y^2 = \tfrac{1}{16}(1 + 32\lambda) + D|y| \qquad (-\infty < D < \infty) \tag{13}$$

They are symmetric under reflection with respect to $x = \frac{1}{4}$ and $y = 0$. For all D they have the same pair of end points $\phi_\pm = \frac{1}{4}(1 \pm \sqrt{1 + 32\lambda})$ which are fixed points of the drift equations. Time increases from ϕ_- to ϕ_+ There is one drift trajectory through each point of the complex plane.

Existence of solution. The drift trajectory consisting of the half-axis $(-\infty, \phi_-)$ is exceptional: any initial point x_0 on this half-axis arrives at $x = -\infty$ in a finite "blowup" time t_0, after which the solution of the drift equations ceases to exist. It is therefore necessary to ask if the solution of the full Langevin equation (4) exists for all times. The same question applies to the equivalent FP equation (with, say, an initial value $F(x, y, 0)$ nonzero only in a finite domain). We consider proving the existence of $F(x, y, t)$ (and of averages such as $\langle\phi\rangle$ and $\langle \mathrm{e}^{-2\phi}\rangle$) beyond the blowup time as a difficult open problem. The physicist's "proof" consists of remarking that the trajectory $\phi(t) = x(t) + \mathrm{i}y(t)$ generated by the Langevin equation never ends, but it ignores the fact that the diffusion constant associated with this trajectory may become arbitrarily large. In any case, a possible singularity that would appear at the blowup time would certainly not represent a physical effect, but only be a property of the particular Poisson representation. We return briefly to these questions in Sec. 8 when considering the special case $\lambda = 0$.

5 Equilibrium

It is easy to verify that the master equation (2) has two independent equilibrium solutions, *viz.* Poissonians of parameter $\sqrt{2\lambda}$ of which one is restricted to the even and the other to the odd nonnegative integers. By superposing these solutions one may write an arbitrary equilibrium solution $P^{\rm eq}(n)$ as

$$P^{\rm eq}(n) = A\, p_{\sqrt{2\lambda}}(n) \,+\, B\, p_{-\sqrt{2\lambda}}(n) \tag{14}$$

The coefficients A and B are determined by the constant of the motion $\mathcal{P}$ according to

$$A = \frac{{\rm e}^{2\sqrt{2\lambda}} \,-\, \mathcal{P}}{2\sinh 2\sqrt{2\lambda}} \qquad B = \frac{-{\rm e}^{-2\sqrt{2\lambda}} \,+\, \mathcal{P}}{2\sinh 2\sqrt{2\lambda}} \tag{15}$$

so that $A + B = 1$ as required by normalization. An obvious way to Poisson represent the equilibrium solution (14) is

$$F^{\rm eq}(x,y) \;=\; \delta(y) F_1^{\rm eq}(x) \tag{16}$$

with

$$F_1^{\rm eq}(x) \;=\; A\,\delta(x - \sqrt{2\lambda}) \,+\, B\,\delta(x + \sqrt{2\lambda}) \tag{17}$$

Two limiting cases merit special consideration. For $\lambda \to \infty$ the coefficient B vanishes exponentially and the equilibrium solution (17) approaches $\delta(x - \sqrt{2\lambda})$. The limit $\lambda \to 0$ is singular (the two delta peaks in Eq. (17) coalesce) and requires separate analysis. In the n representation one has in this limit

$$P^{\rm eq}(n) = \tfrac{1}{2}(1 + \mathcal{P})\,\delta_{n0} \,+\, \tfrac{1}{2}(1 - \mathcal{P})\,\delta_{n1} \tag{18}$$

in agreement with the fact that for $\lambda = 0$ there remains 0 or 1 particle, depending on the initial state. One possible Poisson representation of (18) is

$$F_1^{\rm eq}(x) = \tfrac{1}{2}(1 + \mathcal{P})\,\delta(x) \,-\, \tfrac{1}{2}(1 - \mathcal{P})\,\frac{\rm d}{{\rm d}x}\delta(x) \tag{19}$$

as is easily verified by substitution in Eq. (3). The second term in Eq. (19) is no longer nonnegative, and hence in this case $F_1^{\rm eq}$ is actually a quasi-probability distribution. We emphasize that the Poisson representations exhibited here are by no means unique. Below we will see how other representations of the equilibrium distributions arise.

6 Approach of equilibrium

The approach of equilibrium in the n representation is very unsurprising. For $t \to \infty$ the distribution $P(n,t)$ will tend to an equilibrium $P^{\rm eq}(n)$ uniquely determined by the initial value of $\mathcal{P}$ and given by (14)–(15).

We will now consider the approach to equilibrium in the ϕ representation for an initial state $\phi(0) = \rho$, *i.e.* for an initial Poisson distribution $P(n,0) = p_\rho(n)$. The constant of the motion then has the value $\langle(-1)^n\rangle = {\rm e}^{-2\rho}$. We are led to distinguish two cases.

Real solutions. Let us first suppose that the initial value ρ is in the interval $[-\sqrt{2\lambda}, \sqrt{2\lambda}]$. In this case the time dependent probability distribution $F(x,t)$ of ϕ on this interval is described by the equivalent FP equation (7) For $\lambda > 0$ the two boundary points are "adhesive" (in the terminology of Ref. [13]). For $t \to \infty$ the solution tends to the equilibrium distribution $F^{\rm eq}(x)$ given by (17) and (15) with $\langle(-1)^n\rangle = {\rm e}^{-2\rho}$. Note that when ρ is in the interval under consideration, we have $A,\, B \geq 0$.

Complex solutions. Let now ρ be real but outside $[-\sqrt{2\lambda}, \sqrt{2\lambda}]$ (only $\rho > \sqrt{2\lambda}$ is physical). The Langevin equation (4) then generates a stochastic trajectory $\phi(t)$ in the complex plane. The time evolution is equivalently described in this case by an FP equation for the *bivariate* probability distribution $F(x,y,t)$ with initial condition $F(x,y,0) = \delta(y)\delta(x - \rho)$. Since in this case either A or B is negative, the – necessarily nonnegative – solution $F(x,y,t)$ cannot for $t \to \infty$ tend to the double delta peak given by

(16)–(17). Hence something else must happen. In fact, for $t \to \infty$ the distribution $F(x, y, t)$ tends to a stationary distribution $F^{\rm eq}$ that has its support in the complex plane. To obtain this distribution, we have let a set (a "cloud") of 10 000 points, initially all concentrated in $\phi = 1$, evolve independently in time, until their spatial distribution had reached (or, at least, closely approached) a stationary state, that we identify with $F^{\rm eq}$. The resulting final cloud is shown in Fig. 2 for the special cases $\lambda = 0$ and $\lambda \to \infty$, where for the latter we have shifted the origin according to $x = \sqrt{2\lambda} + u$. The distributions $F^{\rm eq}$ for $0 < \lambda < \infty$ interpolate smoothly between these two limiting cases. They are Poisson representations of (14) distinct from (17). To our knowledge this is the first time that such equilibrium distributions in the complex plane have been explicitly determined numerically. Because of the initial condition the distributions shown here are characterized by the constants of the motion $\langle {\rm e}^{-2\phi} \rangle = {\rm e}^{-2}$ and $\langle {\rm e}^{-2\chi} \rangle = {\rm e}^{-2}$. However, different values of the constants of the motion yield almost identical (*i.e.* visually indistinguishable) distributions; this is because the value of the constant of the motion may be changed arbitrarily by a slight redistribution of the probability density faraway in the left half plane.

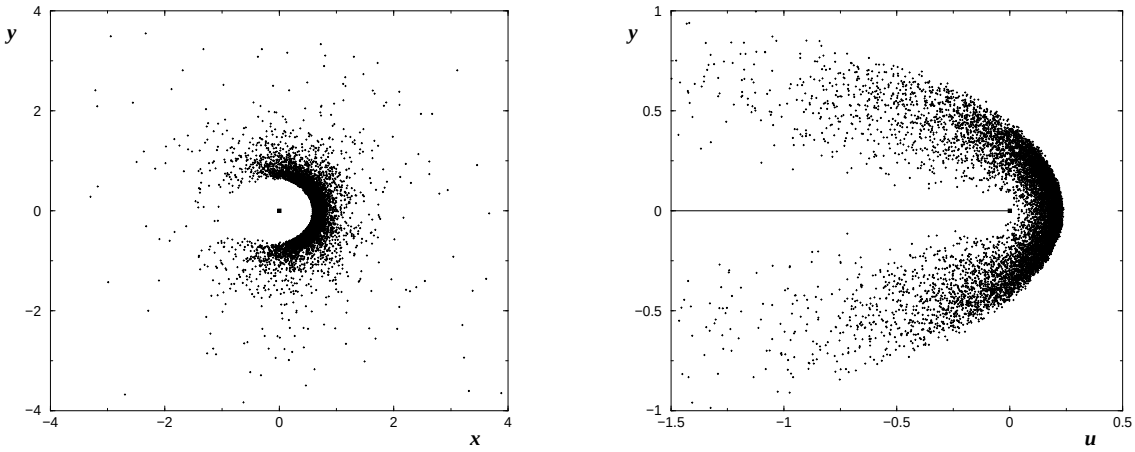

Figure 2: *Left:* Cloud of 10 000 points representing the stationary probability distribution $F^{\rm eq}(x, y)$ in the complex plane $\phi = x + {\rm i}y$ for $\lambda = 0$. *Right:* Cloud of 10 000 points representing $F^{\rm eq}(u, y)$ in the complex plane $\chi = u + {\rm i}y$ for $\lambda = \infty$.

7 Limit $\lambda \to \infty$

We set $\phi = \sqrt{2\lambda} + \chi$ with $\chi = \sqrt{2\lambda} + u + {\rm i}y$ and scale time according to $\tau = \sqrt{2\lambda}\, t$. The limit $\lambda \to \infty$ of (4) then exists and χ satisfies the Langevin equation

$$\frac{{\rm d}\chi}{{\rm d}\tau} = -2\chi + \sqrt{-2\chi}\,\zeta(\tau) \qquad [\,{\rm I}\,] \tag{20}$$

where $\langle \zeta(\tau)\zeta(\tau') \rangle = \delta(\tau - \tau')$. This equation conserves the average $\langle {\rm e}^{-2\chi} \rangle$. It is interesting to remark that in this limit the drift equation has become linear so that the problem of blowup in finite time, discussed in Sec. 4, has disappeared. Below we will continue to use the symbols F_1 and F for probability densities on the u axis and in the uy plane, respectively.

Real solutions. When χ is real and negative, we merely have a limiting case of the real problem discussed in Sec. 6, but with the advantage that $F_1(u, t)$ may be found exactly for arbitrary initial condition

u_0. After obtaining and solving an equation for the Fourier transform of F_1 one finds that $F_1(u,t) = \exp(\frac{2u_0}{\mathrm{e}^{2t}-1})\delta(u) + F_{\mathrm{cont}}(u,t)$. Here $F_{\mathrm{cont}}(u,t)$ is an explicitly known continuous density on the negative u axis which tends to zero with time for all u, while evolving in such a manner that $\langle \mathrm{e}^{-2\chi}\rangle$ remains constant. A similar example of such a solution was worked out in detail in Ref. [13], ch. XII.5.

Complex solutions. Any distribution F not initially confined to the negative u axis spreads out into the complex uy plane. It is then of advantage to transform to the new coordinates $R = \mathrm{Re}\sqrt{4\chi}$ and $Q = \mathrm{Im}\sqrt{4\chi}$, where $R \geq 0$ and $-\infty < Q < \infty$. Up to inessential coefficients these variables are equal to the $\lambda \to \infty$ limits of, respectively, $\mathcal{R}$ and $\mathcal{Q}$ defined in Sec. 4. In terms of R and Q the Langevin equation (20) reads

$$\begin{aligned} \frac{\mathrm{d}R}{\mathrm{d}\tau} &= -R + \frac{R}{R^2+Q^2} \\ \frac{\mathrm{d}Q}{\mathrm{d}\tau} &= -Q - \frac{Q}{R^2+Q^2} + \sqrt{2}\,\zeta(\tau) \end{aligned} \tag{21}$$

which shows that diffusion takes place only parallel to the Q axis. The lines $R = E$, where E is a constant, correspond to the set of parabolas $u = -y^2/E^2 + \frac{1}{4}E^2$ in the uy plane. In spite of this simplification we are not in this case able to explicitly find the stationary density $F^{\mathrm{eq}}(u,y)$, let alone a time dependent solution $F(u,y,t)$. Nevertheless, one sees directly from (21) that $\mathrm{d}R/\mathrm{d}\tau < 0$ outside the circle $Q^2 + R^2 = 1$. Therefore the probability flow across the line $R = 1$ can only be towards the left and the stationary probability density $F^{\mathrm{eq}}(u,y)$ must be identically zero for $R > 1$, *i.e.* for $u + y^2 > \frac{1}{4}$.

8 Limit $\lambda \to 0$

For $\lambda \to 0$ the interval $[-\sqrt{2\lambda}, \sqrt{2\lambda}]$ on which there exists a real solution, contracts to the origin. When $\lambda = 0$ we may set $\phi = r\mathrm{e}^{\mathrm{i}\psi}$ and rewrite the Langevin equation (4) in terms of the polar coordinates,

$$\begin{aligned} \frac{\mathrm{d}r}{\mathrm{d}t} &= \tfrac{1}{2}r - r^2\cos\psi \\ \frac{\mathrm{d}\psi}{\mathrm{d}t} &= -r\sin\psi + \zeta(t) \end{aligned} \tag{22}$$

This shows that diffusion takes place only along the angular direction in the ϕ plane. The origin is a fixed point. Furthermore, since $\mathrm{d}r/\mathrm{d}t > 0$ inside the punctuated disk $0 < r < \frac{1}{2}$, the probability that flows out of this disk cannot reenter it, and the stationary probability density $F^{\mathrm{eq}}(x,y)$, shown in Fig. 3, must be identically zero for $0 < r < \frac{1}{2}$. We remark parenthetically that for $0 < \lambda < \infty$ there are no such regions where F^{eq} vanishes.

For $\lambda = 0$ the Langevin equation (4) becomes linear in terms of the variable ϕ^{-1}. Its solution with initial value $\phi(0) = \phi_0$ may then be given explicitly and reads

$$\phi(t) = \phi_0 \left[\mathrm{e}^{-\frac{t}{2}-\mathrm{i}Z(t)} + \phi_0 \int_0^t \mathrm{d}\tau\; \mathrm{e}^{-\frac{\tau}{2}+\mathrm{i}Z(t-\tau)-\mathrm{i}Z(t)}\right]^{-1} \tag{23}$$

in which $Z(t)$ is the Wiener process

$$Z(t) = \int_0^t \mathrm{d}\tau\,\zeta(\tau) \tag{24}$$

The moments $\langle\phi^m(t)\rangle$ may be calculated from the mth power of expression (23), since after expanding in powers of ϕ_0 it is possible to average all terms in the resulting series explicitly with respect to $Z(t)$. For $t \to \infty$ the moment $\langle\phi^m(t)\rangle$ is found to tend to $\frac{1}{2}\delta_{m1}(1 - \mathrm{e}^{-2\phi_0})$, in agreement with what one may conclude by combining equations (6), (18), (15), and (8). Although these moments appear to exist, the derivation is formal in that it ignores the convergence questions of the series, and hence does not constitute an answer to the existence problem raised at the end of Sec. 4.

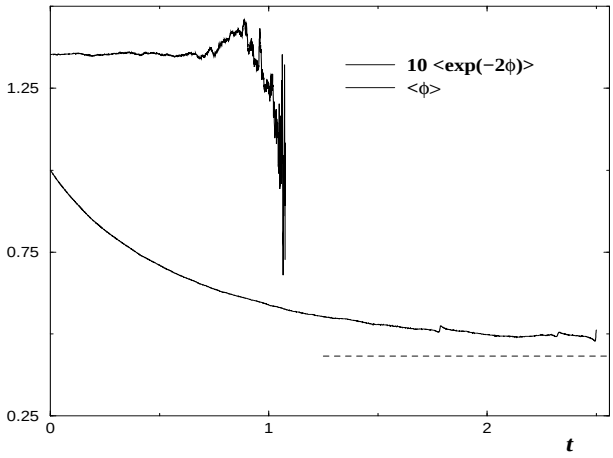

Figure 3: Time evolution of the real part of the average $\langle\phi\rangle$ and the conserved parity $\langle \mathrm{e}^{-2\phi}\rangle = \mathrm{e}^{-2}$, for an initial value $\phi(0) = 1$ and for $\lambda = 0$. The Monte Carlo average is on 10 000 realizations of the stochastic process. The dashed line indicates the theoretical equilibrium average $\langle\phi\rangle = \frac{1}{2}(1 - \mathrm{e}^{-2}) = 0.4323\ldots$ for this initial condition.

9 Remarks on numerical simulation

It is natural to ask if simulating the Langevin equation for the field ϕ has any advantages over simulating a particle system. Numerical integration of the Langevin equation (4) may be carried out on a "cloud" of points in the complex ϕ plane, representative of the function $F(x, y, t)$. We illustrate below by means of two examples two different statistical problems that one encounters, depending on the choice of Poisson representation.

Problems associated with large $|\phi|$. Fig. 3 shows, for the special case $\lambda = 0$, the time evolution of the average $\langle\phi\rangle$ and the constant of the motion $\langle \mathrm{e}^{-2\phi}\rangle$ associated with a cloud of 10 000 points initially all concentrated in $\phi = 1$. For $t > 0$ this cloud spreads out and its average position starts moving. The initial decay of $\langle\phi\rangle$ and the constancy of $\langle \mathrm{e}^{-2\phi}\rangle$ are in full agreement with what we know analytically. After a relatively short time it will begin to happen that occasionally one of the points in the cloud moves to large negative values of x, after which it quickly returns via a large loop to a faraway region near the positive x axis. These large excursions, when they begin to occur, dominate and distort the averages, which then become erratic. In Fig. 3 this happens for $\langle\phi\rangle$ when $t \gtrsim 2.5$, and for the more sensitive average $\langle \mathrm{e}^{-2\phi}\rangle$ when $t \gtrsim 1$.

For the initial condition $\phi = 1$ the average $\langle\phi\rangle$ should for $t \to \infty$ tend exponentially to its equilibrium value $\langle\phi\rangle = \frac{1}{2}(1 - \mathrm{e}^{-2})$. In reality, due to accumulating errors, it ends up by fluctuating around $\frac{1}{2}$. The reason for this value is that after having made a large loop, the trajectories $\phi(t)$ arrive at large x values that are close to even or odd n's with the same probability. Hence the numerical errors cause a "leak" between the two invariant subspaces ("parity violation") which redistributes the total probability equally over both. We have not in this study attempted to control these numerical errors.

One ultimate interest is the solution of problems with diffusion, *i.e.*, for the case with $\lambda = 0$, of the system of coupled Langevin equations

$$\frac{\mathrm{d}\phi_j}{\mathrm{d}t} = \mathsf{D}\,\Delta\phi_j - \phi_j^2 + \mathrm{i}\phi_j\,\zeta_j(t) \qquad [\,\mathrm{I}\,] \tag{25}$$

where D is the diffusion constant, j a lattice site index and Δ the lattice Laplacian. The fact that in the Poisson representation the diffusion process is deterministic, suggests that Eq. (25) might be a good starting point for numerical simulation: a part of the problem's stochastic character has been eliminated. Moreover, upon passing from the single site problem discussed so far to the lattice problem (25), one might

think that the diffusion term, because it tends to equalize the ϕ_j, would attenuate the effect of excursions deep into the negative half plane. Actual simulations show that for large enough D indeed it does, but this advantage is offset by the the fact that the asymptotic decay of the particle density (well-known to be as $t^{-1/2}$) then also sets in later.

Problems associated with small $|\phi|$. All Monte Carlo simulations discussed above concerned real positive probability distributions $F(x, y, t)$. As remarked in Sec. 2, a Poisson representation may also be realized with the aid of a quasi-probability, *i.e.* a function F that may take negative (or even complex) values. The time evolution of such quasi-probabilities may also, in principle, be obtained from the Monte Carlo simulation of the Langevin equation. We show this on the example of a state with initially exactly N particles. Such a state may be Poisson represented by $F(x, y) = \delta(y)F_1(x)$ where $F_1(x)$ is the quasi-probability distribution

$$F_1(x) = \mathrm{e}^x \left(-\frac{\mathrm{d}}{\mathrm{d}x}\right)^N \delta(x) \tag{26}$$

as is easily verified by substitution in Eq. (3). (An alternative formula uses a representation on a circle of radius ϵ around the origin; we do not discuss this here.) In order to be able to work numerically with Eq. (26) we express the derivative of the Dirac delta as

$$\frac{\mathrm{d}}{\mathrm{d}x}\delta(x) = \frac{1}{\epsilon}\left[\,\delta(x - \tfrac{1}{2}\epsilon) - \delta(x + \tfrac{1}{2}\epsilon)\,\right] \tag{27}$$

where ϵ should be taken sufficiently small to have a good approximation. N-fold application of Eq. (27) yields the Nth derivative as a sum of $N+1$ delta functions. Combining this with Eq. (26) one obtains for the special case of $N = 4$

$$F_1(x) = \frac{1}{\epsilon^4}\left[\,\mathrm{e}^{2\epsilon}\delta(x - 2\epsilon) - 4\mathrm{e}^{\epsilon}\delta(x - \epsilon) + 6\delta(x) - 4\mathrm{e}^{-\epsilon}\delta(x + \epsilon) + \mathrm{e}^{-2\epsilon}\delta(x + 2\epsilon)\,\right] \tag{28}$$

This representation has its support confined within a circle of arbitrarily small radius around the origin in the complex plane. We have carried out a simulation of the time evolution of the initial state (28) taking $\epsilon = 0.01$ and representing the initial state by four clouds of 10 000 points each. The two located in $x = \pm\epsilon$ each have weight $-4\mathrm{e}^{\pm\epsilon}$ and those in $x = \pm 2\epsilon$ have weight $\mathrm{e}^{\pm 2\epsilon}$. Since the FP equation for $F(x, y, t)$ is linear, these weights stay attached to the clouds during their time evolution. A trivial cloud with weight 6 is located in $x = 0$; it does not move with time, so need not be simulated, but enters into the calculation of averages.

We have taken $\lambda = 0$. Fig. 4 shows the decay of the initial state with $N = 4$ particles. The curves do not change when ϵ is taken smaller. Again, after a relatively short time strong fluctuations appear and the result becomes unreliable. This instability is due to the fact that the fourth derivative in Eq. (28) involves the four times repeated subtraction of almost equal numbers. This explanation is confirmed by the fact that for $N = 2$ the instability appears at a later time, as shown for comparison in Fig. 4.

Another new feature appears in this representation. Since ϵ is arbitrarily small and the radial time derivative $\mathrm{d}r/\mathrm{d}t$ is bounded from above, as shown by the first one of Eqs. (22), the clouds of points will reach the circle $r = \frac{1}{2}$ only after a time T_ϵ that diverges as $\epsilon \to 0$, *i.e.*, after the process has come arbitrarily close to equilibrium. Hence in the limit $\epsilon \to 0$ the decay to the physical equilibrium takes place inside the disk $|\phi(t)| < \frac{1}{2}$, even though the equilibrium distribution $P^{\mathrm{eq}}(n)$ is represented by a *nonstationary* $F(x, y, t)$ inside this disk. This simulation is probably closest to the analytical treatment of field theory, which amounts to working with ϕ close to zero.

10 Final comments

We have performed a case study – to our knowledge the first of its kind – of various analytical and simulational aspects of reaction–diffusion processes in the Poisson representation. We have identified

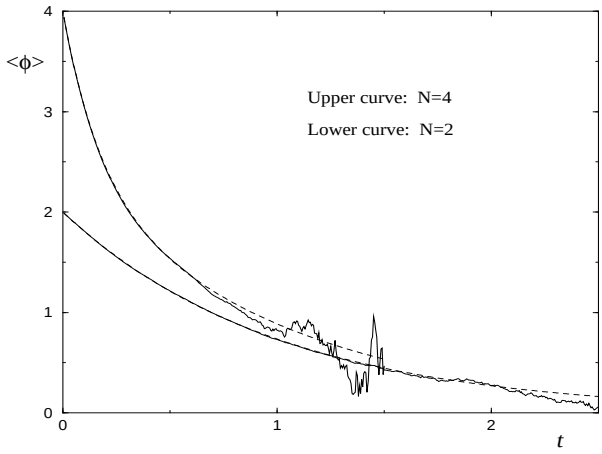

Figure 4: Time evolution of the Monte Carlo averages $\langle\phi\rangle$ for initial states with $N = 4$ and $N = 2$ particles. The dashed curves represent the exact solutions.

many curious and interesting phenomena that happen to the probability flow in this representation. This study is an exploration, and necessarily far from exhaustive. We have not discussed, for example, the equilibrium fluctuations that occur when $\lambda > 0$. One of our motivations was the search for different and possibly more efficient Monte Carlo simulation methods for such processes. It seems clear that such a hope is not easily realized. A more speculative perspective is a combination of the present kind of Monte Carlo simulation with renormalization.

Acknowledgments

The authors have benefitted from discussions with F. van Wijland and from correspondence with M. Droz.

References

[1] C. W. Gardiner, *Handbook of Stochastic Methods*, 2nd edition (Springer, Berlin 1990).

[2] J. L. Cardy in: *The Mathematical Beauty of Physics,* eds. J.-M. Drouffe and J.-B. Zuber (World Scientific, Singapore 1996).

[3] K. Park, H. Hinrichsen, and I. Kim, *Phys. Rev. E* **63** (2001) 065103.

[4] B. P. Lee, *J. Phys. A* **27** (1994) 2633.

[5] P.-A. Rey and J. L. Cardy, *J. Phys. A* **32** (1999) 1585.

[6] M. J. Howard and U. C. Täuber, *J. Phys. A* **30** (1997) 7721.

[7] M. Doi, *J. Phys. A* **9** (1976) 1465.

[8] L. Peliti, *J. Physique* **46** (1985) 1469.

[9] B. P. Lee and J. L. Cardy, *J. Stat. Phys.* **80** (1995) 971.

[10] M. Droz and A. McKane, *J. Phys. A* **27** (1994) L467.

[11] H. Risken, *The Fokker–Planck equation* (Springer, Berlin 1989).

[12] F. van Wijland, *Phys. Rev. E* **63** (2001) 022101.

[13] N. G. van Kampen, *Stochastic Processes in Physics and Chemistry* (North-Holland, Amsterdam 1992).